

A Unified Model of the Prompt Optical Emission of Gamma-Ray Bursts

Hirotsugu Doi¹, Kentaro Takami¹, and Ryo Yamazaki¹

ABSTRACT

The observational diversity of optical emission, which coincides with prompt gamma-ray bursts (GRBs), has been discovered in the recent *Swift* era. We show that on the assumption of the synchrotron radiation for the observed energy range below the X-ray band, the observed diversity can be explained using the internal shock model by taking into account a high-latitude emission and the spectral change due to the synchrotron self-absorption. It may even be possible in our model to include bright optical flashes found, e.g., in GRB 990123. The prediction of our model is that the spectral index in the optical band is dependent on whether the optical light curve correlates with those in the X-rays and/or γ -rays or not, which will be tested in the near future.

Subject headings: gamma rays: bursts — gamma rays: theory

1. Introduction

Thanks to *Swift* observations, γ -ray bursts (GRBs) can be rapidly followed-up in various observation bands (see Zhang 2007, for a recent review). In particular, some events have been observed in the optical band during the prompt γ -ray-active phase (e.g., Yost et al. 2006; Rykoff et al. 2006; Roming et al. 2006). There is observational diversity in the prompt optical emission and several categories can be found as described in the following:

(i) The optical light curve synchronizes with the X-ray/ γ -ray light curve with the optical-to-X/ γ -ray flux ratio almost constant with time (e.g., GRB 041219a; Vestrand et al. 2005). The peak flux ratio $R_{\text{peak}} = F_{\nu_R}^{\text{peak}}/F_{\nu_X}^{\text{peak}}$ is from a few to ten.

¹ Department of Physical Science, Hiroshima University, Higashi-Hiroshima, Hiroshima 739-8526, Japan; doi@theo.phys.sci.hiroshima-u.ac.jp, takami@theo.phys.sci.hiroshima-u.ac.jp, ryo@theo.phys.sci.hiroshima-u.ac.jp.

(ii) The optical light curve is smooth and much less variable compared with X-ray/ γ -ray light curve (e.g., GRB 060210; Stanek et al. 2007). The peak flux ratio R_{peak} is almost equal to or smaller than unity for GRB 060210.

(iii) The optical light curve is a superposition of a smooth component and a variable one synchronizing with X-ray/ γ -ray light curves (e.g., GRB 050820A; Vestrand et al. 2006). This may be an intermediate case between cases (i) and (ii).

(iv) A few events show bright optical flashes just after the γ -ray-active phase. A typical example is GRB 990123 (Akerlof et al. 1999), and for this event $R_{\text{peak}} \sim 2 \times 10^2$ (Briggs et al. 1999). GRB 060111B may also be in this class (Klotz et al. 2006).

(v) For a fraction of the events, UVOT on *Swift* detected no optical counterpart within 10^3 sec after the BAT trigger, and it gave strict upper limits on the prompt optical emission (Roming et al. 2006). Although it is difficult to discuss quantitatively, some events may have dim prompt optical emission.

The origin of the prompt optical emission has been widely discussed (e.g., Panaitescu & Mészáros 2000; Fan et al. 2005; Wei 2007; Panaitescu & Kumar 2006). The popular interpretation is that of case (i), which postulates an internal shock origin (Vestrand et al. 2005), while case (iv) postulates an external reverse shock emission origin (e.g., Sari & Piran 1999; Mészáros & Rees 1999; Wang et al. 2000; Zhang et al. 2003; Nakar & Piran 2004; McMahon et al. 2006). Case (iii) is a superposition of both components. In this Letter, however, we will show that all of the cases are explained in the internal shock model.

2. Prompt emission model and optical/X-ray light curves

Basically, we adopt the same model as in the previous works (Yamazaki et al. 2004; Toma et al. 2005a,b). However, in this Letter, a much simplified version is considered. The central engine launches N_{tot} -emitting shells in the same direction, with the Lorentz factor $\gamma = (1 - \beta^2)^{-1/2}$ and the opening half-angle of $\Delta\theta_{\text{tot}}$. We introduce the spherical coordinate system $(t, r, \vartheta, \varphi)$ in the central engine frame, where the origin is the location of the central engine and $\vartheta = 0$ is the axis of the whole jet. We assume that an observer sees the jet on-beam (i.e., in notation of our previous works, $\Delta\theta_{\text{sub}}^{(j)} = \Delta\theta_{\text{tot}}$, $\vartheta^{(j)} = 0$, and $\vartheta_{\text{obs}} = \theta_v^{(j)} = 0$, then $\Delta\phi^{(j)} = \pi$). The departure time of each emitting shell $t_{\text{dep}}^{(j)}$ is assumed to be homogeneously random between $t = 0$ and $t = t_{\text{dur}}$, where t_{dur} is the duration time of the central engine in its own frame. The jet emission instantaneously arises at $r = r_0$. Then the observed flux $F_\nu(T)$ at an observer time T and at an observed frequency ν is a superposition of each shell

emission calculated as (Toma et al. 2005b)

$$F_{\nu}^{(j)}(T) = K_0 \tau_{(j)}^{-2} f(\tau_{(j)} \nu / \gamma) \quad , \quad (1)$$

where

$$\tau_{(j)} = (c\gamma^2 / r_0)(T - t_{\text{dep}}^{(j)}) \quad (2)$$

and K_0 is the normalization constant. Here $T = 0$ is chosen as the time of arrival at the observer of a photon emitted at the origin at $t = 0$. In our model, synchrotron radiation is considered. Assuming the standard internal shock model and typical model parameters, the break frequencies at the on-beam observer are calculated as $\nu_m \sim 30$ keV and $\nu_a \sim 10$ eV, where we assume the bulk Lorentz factor $\Gamma = 300$, the Lorentz factor of the internal shock $\Gamma_{sh} = 5$, the outflow luminosity $L_m = 1 \times 10^{52}$ erg s⁻¹, the observed typical variability timescale $\delta t = 1$ sec, and the shock microphysics parameters $\varepsilon_e = \varepsilon_B = 0.5$ (see eqs.(1)–(3) in Wei 2007). The cooling frequency at the on-beam observer ν_c is found to be much smaller than ν_a . Note that considering several uncertainties of the parameters arising in the internal shock model, ν_a could be around the R-band frequency $\nu_R = 1.7$ eV. Then the spectral shape function, $f(\nu')$, is given by (e.g., Panaitescu & Mészáros 2000; Fan & Wei 2004)

$$f(\nu') = \begin{cases} (\nu' / \nu'_a)^{5/2} & (\nu' < \nu'_a) \\ (\nu' / \nu'_a)^{-1/2} & (\nu'_a < \nu' < \nu'_m) \\ (\nu'_m / \nu'_a)^{-1/2} (\nu' / \nu'_m)^{-p/2} & (\nu'_m < \nu') \end{cases} \quad , \quad (3)$$

which is different from that for the case $\nu'_a < \nu'_c < \nu'_m$ (Sari et al. 1998). One should remark that for $\nu' < \nu'_a$, $f(\nu')$ has a steep slope because of the synchrotron self-absorption. We don't consider the spectrum in the range $\nu' < \nu'_c$ in Eq. (3), because we assume $\nu'_c \ll \nu'_a$ based on the above order-of-magnitude estimation and then our result does not depend on the value of ν'_c . In order to more accurately reproduce the observational properties such as R_{peak} , we may have to introduce another emission component that is responsible for the high-energy X-rays and/or γ -rays in the observer frame, whose spectrum is characterized by the Band function (Band et al. 1993). However such a correction is neglected here for simplicity. The pulse starting and ending times of each shell emission are

$$T_{\text{start}}^{(j)} = t_{\text{dep}}^{(j)} + (r_0 / \beta c)(1 - \beta) \quad , \quad (4)$$

$$T_{\text{end}}^{(j)} = t_{\text{dep}}^{(j)} + (r_0 / \beta c)(1 - \beta \cos \Delta\theta_{\text{tot}}) \quad . \quad (5)$$

In this Letter, the cosmological effect is neglected (i.e., we set $z = 0$). In the following, we adopt the fiducial parameters $r_0 = 1 \times 10^{15}$ cm, $\gamma = 100$, $\Delta\theta_{\text{tot}} = 0.25$ rad, $t_{\text{dur}} = 10$ sec, $N_{\text{tot}} = 50$, $\nu'_m = 1$ keV, and $p = 2.5$ unless otherwise stated. We will see how the result changes if we change ν'_a , which ranges between 1×10^{-3} eV and 0.1 eV. We stress that the aim of this Letter is to show that the observed diversity of the prompt optical emission

can possibly be explained by our theoretical model. Therefore, a thorough study of the dependence of the other parameters is beyond the scope of this Letter and of future work.

Before discussing further, one should note that since $f(\nu')$ has a power-law form of $f(\nu') \propto \nu'^\beta$, Eqs. (1) and (2) provide us with

$$F_\nu^{(j)} \propto (T - t_{\text{dep}}^{(j)})^{-2+\beta} \nu^\beta, \quad (6)$$

which is the same form as a well known formula that is believed to describe the steep decay phase in the early X-ray afterglow (Kumar & Panaitescu 2000; Liang et al. 2006; Nousek et al. 2006; O'Brien et al. 2006a; Zhang et al. 2006; Yamazaki et al. 2006; Butler & Kocevski 2006). If the absorption frequency at the observer, ν_a ($\nu_a \sim 2\gamma\nu'_a$ if $T \sim T_{\text{start}}^{(j)}$), is below ν_R , then $\beta = -1/2$ at ν_R , so that $F_\nu^{(j)}$ rapidly decreases with $\tau_{(j)}$. On the other hand, if $\nu_a > \nu_R$, then $\beta = 5/2$ at ν_R , so that one can find $F_\nu^{(j)} \propto \tau_{(j)}^{1/2}$. Keeping this in mind, we expect that the optical behavior for $\nu_a < \nu_R$ is rather different from that for $\nu_R < \nu_a$, and that the observed diversity of prompt optical phenomena arises when ν_a varies across ν_R . In this Letter, we consider $F_{\nu_X=10 \text{ keV}}$ as a representative of the X-ray/ γ -ray light curve because as long as $1 \text{ keV} \lesssim \nu \lesssim 100 \text{ keV}$, the light curve F_ν shows almost the same behavior. The following five cases (i)–(v), correspond to those in § 1:

(i) Let us first consider the case $2\gamma\nu'_a < \nu_R$. In this case, we obtain the light curves in the R-band ($\nu_R = 1.7 \text{ eV}$) and the X-ray band ($\nu_X = 10 \text{ keV}$) as

$$F_{\nu_R}^{(j)} = K_0(\gamma\nu'_a/\nu_R)^{1/2}\tau_{(j)}^{-5/2}, \quad (7)$$

$$F_{\nu_X}^{(j)} = \begin{cases} K_0(\gamma\nu'_a/\nu_X)^{1/2}\tau_{(j)}^{-5/2} & (\tau_{\text{start}} < \tau_{(j)} < \gamma\nu'_m/\nu_X) \\ K_0(\nu'_a/\nu'_m)^{1/2}(\gamma\nu'_m/\nu_X)^{p/2}\tau_{(j)}^{-2-p/2} & (\gamma\nu'_m/\nu_X < \tau_{(j)} < \tau_{\text{end}}) \end{cases}, \quad (8)$$

where

$$\tau_{\text{start}} = (c\gamma^2/r_0)(T_{\text{start}} - t_{\text{dep}}^{(j)}) = 1/2, \quad (9)$$

$$\tau_{\text{end}} = (c\gamma^2/r_0)(T_{\text{end}} - t_{\text{dep}}^{(j)}) = [1 + (\gamma\Delta\theta_{\text{tot}})^2]/2, \quad (10)$$

and we use the approximation $1 - \beta \sim 1/2\gamma^2$. Hence, both the optical and the X-ray light curves show rapid decay after the initial sudden rise, so that the optical behavior is similar to the X-ray behavior. When $N_{\text{tot}} \gg 1$, we see many spikes as observed for typical bursts. In particular, the time of the maximum flux is the same in the optical and the X-ray bands. In Figure 1a, we chose $\nu'_a = 1 \times 10^{-3} \text{ eV}$ with other parameters being fiducial. The peak flux ratio is estimated as $R_{\text{peak}} = F_{\nu_R}^{\text{peak}}/F_{\nu_X}^{\text{peak}} \sim (\nu_X/\nu_R)^{1/2} \sim 10^2$, which is larger than the observed value. If we consider the additional Band function component which dominates only in the observed X-ray and γ -ray bands, the value of R_{peak} (\sim several tens) can be closer to the observed one.

(ii) Next we consider the case $\nu_R < 2\gamma\nu'_a$. Then we derive

$$F_{\nu_R}^{(j)} = \begin{cases} K_0(\nu_R/\gamma\nu'_a)^{5/2}\tau_{(j)}^{1/2} & (\tau_{\text{start}} < \tau_{(j)} < \gamma\nu'_a/\nu_R) \\ K_0(\gamma\nu'_a/\nu_R)^{1/2}\tau_{(j)}^{-5/2} & (\gamma\nu'_a/\nu_R < \tau_{(j)} < \tau_{\text{end}}) \end{cases}, \quad (11)$$

while the X-ray light curve is again described by Eq. (8). The optical light curve has a gradually increasing part whose duration is $\sim (\gamma\nu'_a/\nu_R)(r_0/c\gamma^2)$. In particular, in the case of $t_{\text{dur}} \lesssim (\gamma\nu'_a/\nu_R)(r_0/c\gamma^2)$, the difference between optical and X-ray behavior becomes significant. If $N_{\text{tot}} \gg 1$ and $t_{\text{dur}} \lesssim (\gamma\nu'_a/\nu_R)(r_0/c\gamma^2)$, all components are overlaid with each other at the time interval $t_{\text{dur}} \lesssim T \lesssim (\gamma\nu'_a/\nu_R)(r_0/c\gamma^2)$, resulting in a smooth light curve. On the other hand, since an X-ray light curve has short-duration, rapidly decaying pulses, we see less of a superposition effect than we do in the optical case. In Figure 1b, we chose $\nu'_a = 0.1$ eV with other fiducial parameters. One can see that the peak flux ratio is $R_{\text{peak}} \sim O(1)$, which is roughly consistent with the observation.

(iii) In the intermediate case $\nu_R \lesssim 2\gamma\nu'_a$, we can see optical pulses synchronizing with the X-ray/ γ -ray pulses overlaid by a smooth component. In Figure 1c, we chose $\nu'_a = 0.02$ eV with other fiducial parameters.

(iv) In the case of $\nu_R < 2\gamma\nu'_a$, our model can also reproduce bright optical flash associated with e.g., GRB 990123. In Figure 1d, we chose $r_0 = 3 \times 10^{15}$ cm, $\nu'_m = 1$ eV, and $\nu'_a = 0.05$ eV with other fiducial parameters. Since $\gamma\nu'_m \ll \nu_X = 10$ keV, the spectrum at ν_X enters into the regime $\nu'_m < \nu'$ in Eq. (3), resulting in the smaller observed X-ray flux F_{ν_X} compared with cases (i)–(iii). Then the large value of observed R_{peak} can be reproduced. Our result implies that external reverse shock emission is not necessarily required. Recently, Panaitescu & Kumar (2006) proposed a synchrotron-inverse Compton model to explain simultaneously the optical flash and the γ -ray behavior of GRB 990123, which is similar claim as ours. Note that since $\nu'_m = 1$ eV, an additional Band function component is necessary in order to match the observed spectrum in the range $\nu > \nu_X$. Such a correction can be possible without changing the value of $R_{\text{peak}} \sim 10^2$.

(v) Finally, if $\nu_R \ll 2\gamma\nu'_a$, then the observed flux in the optical band becomes dim because of the steep slope below ν_a via the synchrotron self-absorption.

3. Discussion

In this Letter, assuming the synchrotron radiation with the absorption frequency ν_a around the R-band frequency ν_R , we have shown that the observed diversity of the prompt optical emission arises when ν_a varies and that our theoretical model explains the observa-

tion well. At present, the broad-band spectrum of the prompt emission of the GRB is unknown, and several possibilities have been proposed (e.g., Li & Song 2004; Zou et al. 2006; Panaitescu & Kumar 2006). Our discussion can be generalized for such cases. If the comoving spectral function, $f(\nu')$, has the following form around a break frequency $\nu'_b \sim \nu_R/\gamma$,

$$f(\nu') \approx \begin{cases} (\nu'/\nu'_b)^s & (\nu' < \nu'_b) \\ (\nu'/\nu'_b)^q & (\nu'_b < \nu') \end{cases}, \quad (12)$$

where $s \gtrsim 2$ and $q \lesssim 0$, then, our conclusion derived in this Letter remains unchanged qualitatively.

Our model will be tested by observing the spectral energy index, β_O , in the optical band. When the optical light curve synchronizes with the X-ray/ γ -rays (i.e., $\nu_b \approx 2\gamma\nu'_b < \nu_R$), then the optical band is above the break frequency, ν_b , so that the energy index is $\beta_O \approx q \lesssim 0$. On the other hand, if the optical light curve is rather smooth and does not synchronize with the X-ray/ γ -rays light curves, then the optical band is below ν_b ($\nu_R < \nu_b$). Therefore, $\beta_O \approx s \gtrsim 2$ is expected. Therefore, multicolor observation in the optical (and/or infrared) band is important to test our model.

We would like to thank the anonymous referee and K. Ioka for useful comments. This work was supported by Grant-in-Aid for Scientific Research of the Japanese Ministry of Education, Culture, Sports, Science and Technology, 18740153 (R. Y.).

REFERENCES

- Akerlof, C. et al. 1999, *Nature*, 398, 400
- Band, D. L. et al. 1993, *ApJ*, 413, 281
- Briggs, M. S. et al. 1999, *ApJ*, 524, 82
- Butler, N. R. & Kocevski, D. 2006, astro-ph/0612564
- Fan, Y. Z. & Wei, D. M. 2004, *ApJ*, 615, L69
- Fan, Y. Z., Zhang, B., & Wei, D. M. 2005, *ApJ*, 628, L25
- Klotz, A. et al. 2006, *A&A*, 451, L39
- Kumar, P. & Panaitescu, A. 2000, *ApJ*, 541, L51

- Li, Z. & Song, L. M. 2004, *ApJ*, 608, L17
- Liang, E. W., et al. 2006, *ApJ*, 646, 351
- McMahon, E., Kumar, P., & Piran, T. 2006, *MNRAS*, 366, 575
- Mészáros, P. & Rees, M. 1999, *MNRAS*, 306, L39
- Nakar, E. & Piran, T. 2004, *MNRAS*, 353, 647
- Nousek, J. A. et al. 2006, *ApJ*, 642, 389
- O’Brien, P. T. et al. 2006a, *ApJ*, 647, 1213
- Panaitescu, A. & Mészáros, P. 2000, *ApJ*, 544, L17
- Panaitescu, A. & Kumar, P. 2006, *astro-ph/0612504*
- Roming, P. W. A. et al. 2006, *ApJ*, 652, 1416
- Rykoff, E. S. et al. 2006, *ApJ*, 638, L5
- Sari, R., Piran, T., & Narayan, R. 1998, *ApJ*, 497, L17
- Sari, R. & Piran, T. 1999, *ApJ*, 520, 641
- Stanek, K. Z. et al. 2007, *ApJ*, 654, L21
- Toma, K., Yamazaki, R., & Nakamura, T. 2005a, *ApJ*, 620, 835
- Toma, K., Yamazaki, R., & Nakamura, T. 2005b, *ApJ*, 635, 481
- Vestrand, W. T. et al. 2005, *Nature*, 435, 178
- Vestrand, W. T. et al. 2006, *Nature*, 442, 172
- Wang, W. Y., Dai, Z. G., & Lu, T. 2000, *MNRAS*, 319, 1159
- Wei, D. M. 2007, *MNRAS*, 374, 525
- Yamazaki, R., Ioka, K., & Nakamura, T. 2004, *ApJ*, 607, L103
- Yamazaki, R., Toma, K., Ioka, K., & Nakamura, T. 2006, *MNRAS*, 369, 311
- Yost, S. A. et al. 2006, *astro-ph/0611414*
- Zhang, B., Kobayashi, S., & Mészáros, P. 2003, *ApJ*, 595, 950

Zhang, B. et al. 2006, ApJ, 642, 354

Zhang, B. 2007, astro-ph/0701520

Zou, Y. C., Xu, D., & Dai, Z. G. 2006, ApJ, 646, 1098

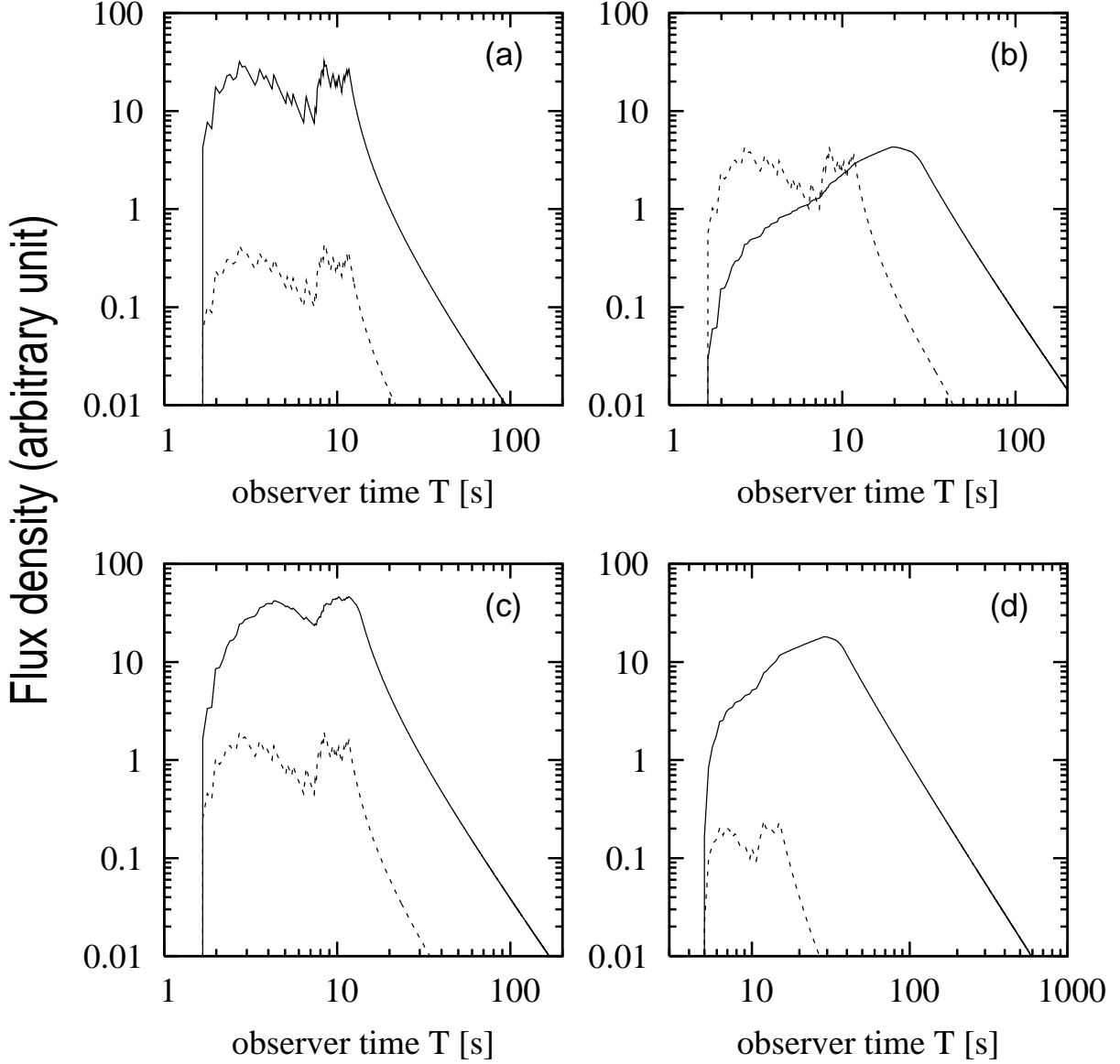


Fig. 1.— Examples of light curves. Solid and dotted lines are for the optical ($\nu_R = 1.7$ eV) and X/ γ -ray ($\nu_X = 10$ keV) bands, respectively. The adopted parameters are (a) $\nu'_a = 1 \times 10^{-3}$ eV, (b) $\nu'_a = 0.1$ eV, (c) $\nu'_a = 0.02$ eV, and (d) $\nu'_a = 0.05$ eV, $\nu'_m = 1$ eV, $r_0 = 3 \times 10^{15}$ cm, with other fiducial parameters ($r_0 = 1 \times 10^{15}$ cm, $\gamma = 100$, $\Delta\theta_{\text{tot}} = 0.25$ rad, $t_{\text{dur}} = 10$ sec, $N_{\text{tot}} = 50$, $\nu'_m = 1$ keV, and $p = 2.5$).